Uzbek Journal "Problems of Mechanics"

Research Article

DOI: 10.68846/pmjournal-2026-37-00007

A Spectral-Grid Method for the Stability Analysis of the Blasius Boundary Layer and the Dynamics of the Velocity Vector

Chori Normurodov[1*], Muhriddin Tilovov[1], Sardorbek Murodov[1], Abdulla Raimov[1], Nasiba Djurayeva[2]

[1] Termez State University, 43 Barkamol Avlod St., Termez, 190111, Uzbekistan
[2] Surkhandarya Academic Lyceum of the Ministry of Internal Affairs, 1 Minor, Jarkurgan, 190613, Uzbekistan
[*] **Corresponding author:** ch.normurodov@gmail.com

Received: 25 June 2026 | **Revised:** 15 August 2026 | **Accepted:** 05 September 2026 | **Published:** 30 September 2026

ABSTRACT

This study investigates the longitudinal and transverse components of linear perturbations in the Blasius boundary layer within the framework of local hydrodynamic stability analysis. The base-flow profile is determined from the Falkner–Skan equation, after which the linearized equations of motion are reduced to the Orr–Sommerfeld spectral problem. For its numerical solution, a spectral-grid method is employed, based on dividing the computational domain into elements and representing the solution on each element by a finite series of Chebyshev polynomials. The resulting generalized eigenvalue problem is reduced to a lower-dimensional system, followed by reconstruction of the eigenvector of the original system and the corresponding eigenfunction. Based on a selected physically relevant mode, the components of the perturbed velocity field are determined. For the test case, the computed eigenvalue is compared with a published reference numerical result; the influence of the distribution of the number of polynomials among the elements of the computational domain is also investigated. The obtained results confirm the applicability of the proposed computational procedure to the analysis of linear perturbations in the Blasius boundary layer.

KEYWORDS

velocity dynamics; Navier–Stokes equations; spectral-grid method; boundary layer; eigenvalues and eigenvectors; stream function

1. Introduction

In [1], a numerical approximation to the classical Blasius boundary-layer problem for flow over a flat plate was obtained using a spectral collocation method. The approach is based on the Chebyshev pseudospectral scheme, in which the solution is approximated by Chebyshev polynomials of the first kind. The Chebyshev pseudospectral method employs Chebyshev–Gauss–Lobatto collocation points corresponding to the extrema of the Chebyshev polynomials. By enforcing the differential equation at these points and incorporating the boundary conditions, the original boundary-value problem is reduced to a system of algebraic equations. The coefficients of the Chebyshev polynomial expansion are then determined to obtain a numerical approximation of the solution.

A new generalized Blasius equation for turbulent flow, derived from the turbulent boundary-layer equation and applicable to both turbulent and laminar flow regimes, was formulated in [2]. Analytical and numerical solutions of the proposed generalized Blasius equation were investigated under prescribed conditions. In fluid mechanics, obtaining analytical solutions to complex systems is generally a labor-intensive and time-consuming process. Therefore, a MATLAB-based numerical procedure was employed to investigate the new third-order nonlinear Blasius equation. The analytical and numerical results were compared using tabulated data and graphical representations in order to verify the validity of the proposed model. According to the authors, the obtained results demonstrated good agreement and were considered promising.

The method proposed in [3] is based on integrating the Orr–Sommerfeld equation from the free stream toward the wall. To satisfy the boundary conditions at the wall, two linearly independent solutions are constructed. The method was applied to calculate the neutral stability curve for the Blasius velocity profile.

In [4], a class of self-similar solutions to the unsteady Navier–Stokes equations was obtained for two-dimensional unsteady laminar flow of a viscous incompressible fluid in the boundary layer over a semi-infinite stationary flat plate. The boundary layer is generated by a uniform free stream over the plate, whereas the unsteadiness of the flow dynamics arises exclusively from the introduced self-similar formulation. For this self-similar solution, the original boundary-layer equations, namely the momentum and heat-transfer equations, are transformed into a system of nonlinear ordinary differential equations involving two physical parameters: the unsteadiness parameter and the Prandtl number. The effects of these parameters on the characteristics of unsteady boundary-layer flow and heat-transfer processes were investigated in detail.

In [5], a free-boundary formulation was proposed for two generalized Blasius problems. The computed values of the so-called missing initial condition were compared with recent results available in the literature and showed good agreement.

In [6], the Blasius equation, which is a third-order nonlinear ordinary differential equation, was transformed into an integral equation with a shifted kernel. The purpose of that study was to develop an efficient modification of the standard Adomian decomposition method combined with the Laplace transform for solving the Blasius equation. One of the main difficulties in solving this problem is that the value of the second derivative at the origin is unknown. Once this derivative is accurately determined, the analytical solution of the Blasius problem can be obtained relatively straightforwardly. Therefore, an approximate solution was used to estimate the second derivative at the origin, commonly referred to as the Blasius constant. Determination of this constant is essential for calculating the wall shear stress on the surface of the plate. Once this value is obtained, the original problem is reduced to an initial-value problem that can subsequently be solved numerically.

New results concerning the classical problem of a viscous, laminar, steady boundary layer of an incompressible Newtonian fluid over a thin flat plate, i.e., the Blasius problem, were presented in [7]. A finite-difference solution of the Blasius problem was obtained using a shooting technique combined with the classical fourth-order Runge–Kutta method over a sufficiently large computational interval with a very fine grid. The numerical results were compared with previously published computational data.

In [8], the classical problem of a viscous laminar boundary layer over a thin flat plate was considered. Using the nonlinear least-squares method, accurate correlations for the streamwise velocity were obtained, which can be used in the numerical simulation of two- and three-dimensional boundary-layer flows. The calculated and analytical velocity profiles were compared with well-established data available in the literature.

In [9], the effectiveness of coordinate mappings for the numerical solution of problems posed on unbounded domains was investigated. Using several model problems, including the Orr–Sommerfeld eigenvalue problem for the Blasius boundary layer and the Falkner–Skan equation, it was demonstrated that such transformations are effective when the solution exhibits relatively simple asymptotic behavior at infinity. The analysis indicated that an algebraic mapping of the infinite domain onto a finite interval is the most preferable approach.

The numerical treatment of a boundary-value problem for a singularly perturbed second-order differential equation was investigated in [10]. The numerical and graphical results demonstrated the high accuracy and computational efficiency of the proposed method.

In [11], an approach to the numerical solution of a boundary-value problem for an inhomogeneous singularly perturbed second-order differential equation was developed based on the continuous version of the pre-integration method.

The numerical modeling of the hydrodynamic stability of a two-phase boundary-layer flow was carried out in [12]. In [13], the hydrodynamic stability of two-phase Poiseuille flow governed by a system of nonlinear singularly perturbed equations was investigated.

In [14], a discrete version of the pre-integration method was proposed for the numerical solution of an inhomogeneous biharmonic equation. The partial derivatives appearing in the equation were represented as finite double expansions in Chebyshev polynomials of the first kind with unknown expansion coefficients. Numerical experiments performed for various test functions confirmed the high accuracy and efficiency of the proposed method. The objective of [15] was to develop a highly accurate and computationally efficient numerical method for investigating the behavior of derivatives of various orders for a singularly perturbed second-order differential equation.

In the present study, the linear stability of the Blasius boundary layer is investigated by applying a spectral-grid method to the Orr–Sommerfeld problem. The computational domain is divided into separate elements, and the unknown function on each element is represented by a finite expansion in Chebyshev polynomials. Particular attention is paid to the formulation of the generalized eigenvalue problem, its subsequent reduction, and the reconstruction of the eigenvector of the original system together with the corresponding eigenfunction. Using the reconstructed eigenfunction, the streamwise and transverse components of the perturbed velocity are determined as solutions of the Navier–Stokes equations linearized about the Blasius base flow. Within this framework, the linear evolution of small perturbations and the structure of the corresponding velocity field are investigated. The computed eigenvalues are compared with published numerical data, and the influence of the distribution of the number of polynomials among the elements of the computational domain on the accuracy of the numerical solution is also examined.

2. Mathematical Model

The motion of a viscous incompressible fluid in dimensionless form is described by the following system of dimensionless Navier–Stokes equations:

$$\begin{aligned}
&\frac{\partial u}{\partial t} + u\frac{\partial u}{\partial x} + \vartheta\frac{\partial u}{\partial y} = -\frac{\partial P}{\partial x} + \frac{1}{\mathrm{Re}}\left(\frac{\partial^2 u}{\partial x^2} + \frac{\partial^2 u}{\partial y^2}\right),\\
&\frac{\partial \vartheta}{\partial t} + u\frac{\partial \vartheta}{\partial x} + \vartheta\frac{\partial \vartheta}{\partial y} = -\frac{\partial P}{\partial y} + \frac{1}{\mathrm{Re}}\left(\frac{\partial^2 \vartheta}{\partial x^2} + \frac{\partial^2 \vartheta}{\partial y^2}\right),\\
&\frac{\partial u}{\partial x} + \frac{\partial \vartheta}{\partial y} = 0.
\end{aligned} \tag{1}$$

where u and ϑ are the streamwise and transverse velocity components, P is the pressure, $\mathrm{Re} = \rho UL/\mu$ is the Reynolds number, ρ is the fluid density, μ is the dynamic viscosity, and U and L are the characteristic velocity and length scales, respectively. For plane Poiseuille flow in a semi-infinite channel, the characteristic length is the half-width of the channel, while the characteristic velocity is $U^{\max}$ at the channel centerline. In a boundary layer, the characteristic length is the boundary-layer thickness and the characteristic velocity is the velocity outside the boundary layer.

The aim of this study is to investigate the streamwise $u(x, y, t)$ and transverse $\vartheta(x, y, t)$ components of the velocity field in the Blasius boundary layer within the framework of linear hydrodynamic stability theory. The velocity components are defined as the sum of the base flow and a small perturbation obtained by solving the Orr–Sommerfeld problem. The space–time domain under consideration is specified as

$$D = \{0 \le x \le 50, \quad 0 \le y < \infty, \quad 0 \le t \le 50\}.$$

For the stability analysis, the flow is represented as a superposition of a steady base flow and a small perturbation:

$$\begin{aligned}
u(x, y, t) &= U(y) + \widetilde{u}(x, y, t),\\
\vartheta(x, y, t) &= \widetilde{\vartheta}(x, y, t),\\
P(x, y, t) &= P(x, y) + \widetilde{p}(x, y, t).
\end{aligned} \tag{2}$$

It is assumed that the perturbation amplitude is much smaller than the characteristic velocity of the base flow, which permits retaining only first-order terms in the perturbations. Substituting expansion (2) into the Navier–Stokes equations (1) and retaining only terms linear in the perturbations yields the linearized system of equations for the perturbed quantities:

$$\frac{\partial \widetilde{u}}{\partial t} + U\frac{\partial \widetilde{u}}{\partial x} + \widetilde{\vartheta}\frac{dU}{dy} = -\frac{\partial P}{\partial x} - \frac{\partial \widetilde{p}}{\partial x} + \frac{1}{\mathrm{Re}}\left(\frac{d^2U}{dy^2} + \Delta\widetilde{u}\right),$$
$$\frac{\partial \widetilde{\vartheta}}{\partial t} + U\frac{\partial \widetilde{\vartheta}}{\partial x} = -\frac{\partial P}{\partial y} - \frac{\partial \widetilde{p}}{\partial y} + \frac{1}{\mathrm{Re}}\Delta\widetilde{\vartheta}, \tag{3}$$
$$\frac{\partial \widetilde{u}}{\partial x} + \frac{\partial \widetilde{\vartheta}}{\partial y} = 0,$$

where

$$\Delta = \frac{\partial^2}{\partial x^2} + \frac{\partial^2}{\partial y^2}.$$

In a local stability analysis, the Blasius profile at a fixed streamwise section $x = x_0$ is treated as quasi-parallel. For the zero-pressure-gradient Blasius flow, we assume

$$\frac{\partial P}{\partial x} = 0, \qquad \frac{\partial P}{\partial y} = 0.$$

Taking into account the assumptions of the local quasi-parallel analysis and eliminating the terms associated with the base flow, system (3) becomes

$$\frac{\partial \widetilde{u}}{\partial t} + U\frac{\partial \widetilde{u}}{\partial x} + \widetilde{\vartheta}\frac{dU}{dy} = -\frac{\partial \widetilde{p}}{\partial x} + \frac{1}{\mathrm{Re}}\Delta\widetilde{u},$$
$$\frac{\partial \widetilde{\vartheta}}{\partial t} + U\frac{\partial \widetilde{\vartheta}}{\partial x} = -\frac{\partial \widetilde{p}}{\partial y} + \frac{1}{\mathrm{Re}}\Delta\widetilde{\vartheta}. \tag{4}$$

$$\frac{\partial \widetilde{u}}{\partial x} + \frac{\partial \widetilde{\vartheta}}{\partial y} = 0. \tag{5}$$

Introduce the streamfunction of the perturbation motion in the form

$$\Psi(x, y, t) = \psi(y)e^{i(kx-\omega t)}. \tag{6}$$

where $\psi(y) = \psi_r + i\psi_i$ is the streamfunction amplitude, k is a real quantity related to the perturbation wavelength by

$$\ell = \frac{2\pi}{k}.$$

The quantity ω is the complex angular frequency

$$\omega = \omega_r + i\omega_i,$$

where ω_r determines the oscillation frequency of the perturbation, whereas ω_i characterizes the rate of change of its amplitude in time. If $\omega_i > 0$, the perturbation amplitude increases, corresponding to flow instability; if $\omega_i < 0$, the perturbations decay and the flow is stable.

In addition to the quantities k and ω, it is useful to introduce their ratio

$$\lambda = \frac{\omega}{k} = \lambda_r + i\lambda_i.$$

The quantity λ_r represents the propagation velocity of the perturbations along the x axis (the phase velocity), whereas λ_i characterizes their growth or decay. If $\lambda_i > 0$, the flow is unstable; if $\lambda_i < 0$, it is stable; and if $\lambda_i = 0$, the perturbations are neutrally stable.

The components of the perturbed velocity are expressed in terms of the streamfunction (6):

$$\widetilde{u}(x, y, t) = \frac{\partial \Psi}{\partial y} = \psi'(y)e^{i(kx-\omega t)}, \qquad \widetilde{\vartheta}(x, y, t) = -\frac{\partial \Psi}{\partial x} = -ik\psi(y)e^{i(kx-\omega t)}. \tag{7}$$

Thus, the continuity equation (5) is satisfied identically. Substituting the obtained expressions into system (4)–(5) and eliminating the pressure yields the spectral problem for the Orr–Sommerfeld equation:

$$\frac{1}{ik\mathrm{Re}}\left(\frac{d^4\psi}{d\eta^4} - 2k^2\frac{d^2\psi}{d\eta^2} + k^4\psi\right) - \left(U(\eta) - \lambda\right)\left(\frac{d^2\psi}{d\eta^2} - k^2\psi\right) + U''(\eta)\psi = 0, \qquad 0 < \eta < \eta_\infty. \tag{8}$$

The boundary conditions correspond to the requirements of impermeability and no-slip:

$$\psi(\eta_0) = \psi'(\eta_0) = 0, \qquad \psi(\eta_\infty) = \psi'(\eta_\infty) = 0.$$

Thus, the stability problem reduces to finding the eigenvalues λ and the corresponding eigenfunctions $\psi(\eta)$.

To solve spectral problem (8), the base-flow velocity profile $U(\eta)$ must be specified. In this study, the base profile is taken as the first derivative of the solution of the Falkner–Skan equation,

$$f''' + ff'' + \beta\left[1 - (f')^2\right] = 0, \qquad 0 \le \eta < \infty, \tag{9}$$

which describes the structure of a laminar boundary layer over a flat plate; that is,

$$U(\eta) = f'(\eta).$$

For Blasius flow, the pressure-gradient parameter is set to $\beta = 0$. In this case, the Falkner–Skan equation (9) takes the form

$$f'''(\eta) + f(\eta) f''(\eta) = 0,$$

with the boundary conditions

$$f(0) = 0, \qquad f'(0) = 0, \qquad f'(\infty) = 1.$$

It should be noted that the Blasius equation is also widely used in the literature in another normalization, namely,

$$g'''(\xi) + \frac{1}{2} g(\xi) g''(\xi) = 0,$$

with the boundary conditions

$$g(0) = 0, \qquad g'(0) = 0, \qquad g'(\infty) = 1,$$

where ξ is the similarity variable corresponding to this normalization. The form of the Blasius equation used in the present study and the classical form given above are related by the transformation

$$\xi = \sqrt{2}\,\eta, \qquad f(\eta) = \frac{1}{\sqrt{2}}\, g(\xi).$$

This transformation gives

$$f'(\eta) = g'(\xi), \qquad f''(\eta) = \sqrt{2}\, g''(\xi).$$

In particular, for $\eta = 0$ we obtain

$$f''(0) = \sqrt{2}\, g''(0).$$

Therefore, the value known for the normalization with coefficient $1/2$,

$$g''(0) \approx 0.332057,$$

corresponds to the value

$$f''(0) = \sqrt{2}\, g''(0) \approx 0.469600$$

in the normalization adopted in the present study.

3. Numerical Model

To determine the base-flow profile numerically, the Blasius problem is solved using a shooting method combined with the classical fourth-order Runge–Kutta method. Since the value of the second derivative $f''(0)$ is not known in advance, it is denoted by

$$s = f''(0).$$

For each trial value of s, the initial-value problem is solved with the initial conditions

$$f(0) = 0, \qquad f'(0) = 0, \qquad f''(0) = s$$

over the finite computational interval

$$0 \le \eta \le \eta_{\max}.$$

The value of s is successively refined so that the numerical solution at the right boundary of the computational domain satisfies the condition

$$f'(\eta_{\max}) = 1.$$

In the numerical calculations, the infinite domain is replaced by the finite interval $0 \le \eta \le \eta_{\max}$, where $\eta_{\max} = 20$. The shooting procedure yields the value

$$f''(0) \approx 0.46959999.$$

After $f''(0)$ has been determined, the Blasius equation is integrated again over the entire computational interval, and the base-flow profile

$$U(\eta) = f'(\eta)$$

is constructed. The resulting profile $U(\eta)$ is then used to formulate the Orr–Sommerfeld spectral problem.

Because different normalizations are used, the parameters of the stability problem must also be converted to a common system of scales. Let Re_1 and k_1 denote, respectively, the Reynolds number and the wavenumber in the normalization used in [9]. When converting to the

normalization adopted in the present study, the corresponding parameters are transformed according to

$$\mathrm{Re} = \sqrt{2}\,\mathrm{Re}_1, \qquad k = \sqrt{2}\,k_1.$$

The resulting values Re and k are subsequently used to formulate the Orr–Sommerfeld spectral problem.

The resulting velocity profile $U(\eta)$ is then interpolated at the Chebyshev collocation points of the first kind and represented by a finite series, as described below.

For this purpose, the function $U(\eta)$ is interpolated at the following nodes of the Chebyshev polynomials of the first kind:

$$y_l = \cos\left(\frac{\pi l}{p_j}\right), \qquad l = 0, 1, \ldots, p_j, \tag{10}$$

where p_j is the number of polynomials used to approximate the solution on the j-th grid element.

The velocity profile can then be represented as a series in Chebyshev polynomials:

$$U_j(y_l) = \sum_{n=0}^{p_j} b_n^{(j)} T_n(y_l), \tag{11}$$

where $T_n(y)$ are Chebyshev polynomials of the first kind, and the coefficients $b_n^{(j)}$ are determined by the formula [12,13]:

$$b_n^{(j)} = \frac{2}{p_j \widetilde{c}_n} \sum_{l=0}^{p_j} \frac{1}{\widetilde{c}_l} U_j(y_l) T_n(y_l), \qquad n = 0, 1, \ldots, p_j, \tag{12}$$

where

$$\widetilde{c}_0 = \widetilde{c}_{p_j} = 2, \qquad \widetilde{c}_l = 1 \quad (l \neq 0, p_j).$$

A spectral-grid method [12,13] is used for the numerical solution of the spectral stability problem. In this method, a uniform or nonuniform grid is introduced in the integration domain. For this purpose, the computational domain $[\eta_0, \eta_N]$ is divided into N elements:

$$[\eta_0, \eta_1], [\eta_1, \eta_2], \ldots, [\eta_{N-1}, \eta_N].$$

Let the solution of the Orr–Sommerfeld equation on the j-th element be denoted by $\psi_j(\eta)$, where $j = 1, 2, \ldots, N$. Then, on each element $[\eta_{j-1}, \eta_j]$, differential equation (8) takes the form [12]:

$$\left(\frac{d^4}{d\eta^4} - 2k^2\frac{d^2}{d\eta^2} + k^4\right)\psi_j - ik\mathrm{Re}\left[(U_j(\eta) - \lambda)D - U_j''(\eta)\right]\psi_j = 0, \qquad j = 1, 2, \ldots, N, \tag{13}$$

where

$$D = \frac{d^2}{d\eta^2} - k^2.$$

The boundary conditions are imposed at the boundaries of the computational domain:

$$\begin{aligned} \psi_1(\eta_0) &= 0, \qquad \frac{d\psi_1}{d\eta}(\eta_0) = 0, \\ \psi_N(\eta_N) &= 0, \qquad \frac{d\psi_N}{d\eta}(\eta_N) = 0. \end{aligned} \tag{14}$$

At the element interfaces, the solution and its derivatives up to the third order must be continuous:

$$\psi_j^{(t)}(\eta_j) = \psi_{j+1}^{(t)}(\eta_j), \qquad t = 0, 1, 2, 3; \qquad j = 1, 2, \ldots, N-1. \tag{15}$$

In the spectral-grid method, each element $[\eta_{j-1}, \eta_j]$ is mapped onto the standard interval $[-1, 1]$. The symbol $y \in [-1, 1]$ is then used as the local Chebyshev coordinate on the standard interval and does not coincide with the physical transverse coordinate of the original formulation. Using the change of variables

$$\eta = \frac{m_j}{2} + \frac{l_j}{2}y, \qquad m_j = \eta_j + \eta_{j-1}, \qquad l_j = \eta_j - \eta_{j-1}.$$

After this transformation, equation (13) takes the form

$$\left(\frac{d^4}{dy^4} - 2k_j^2\frac{d^2}{dy^2} + k_j^4\right)\psi_j - ik_j\mathrm{Re}_j\left[(U_j(y) - \lambda)D_j - U_j''(y)\right]\psi_j = 0, \qquad j = 1, 2, \ldots, N, \tag{16}$$

where

$$D_j = \frac{d^2}{dy^2} - k_j^2, \qquad k_j = \frac{l_j}{2}k, \qquad \mathrm{Re}_j = \frac{l_j}{2}\mathrm{Re}.$$

From the boundary conditions (14) and the continuity conditions (15), we obtain:

$$\psi_1(-1) = 0, \qquad \frac{d\psi_1}{dy}(-1) = 0,$$
$$l_j^{-t}\psi_j^{(t)}(+1) = l_{j+1}^{-t}\psi_{j+1}^{(t)}(-1), \qquad t = 0,1,2,3, \quad j = 1,2,\ldots,N-1, \tag{17}$$
$$\psi_N(+1) = 0, \qquad \frac{d\psi_N}{dy}(+1) = 0.$$

Thus, the original problem (8) is reduced to a spectral-grid approximation of the Orr–Sommerfeld equation (16)–(17) on each element of the computational domain.

For convenience, equation (16) is written in operator form

$$L_j\psi_j = 0, \qquad j = 1,2,\ldots,N, \tag{18}$$

where L_j is the differential operator defined by

$$L_j = \left(\frac{d^4}{dy^4} - 2k_j^2\frac{d^2}{dy^2} + k_j^4\right) - ik_j\mathrm{Re}_j\left[\left(U_j(y) - \lambda\right)D_j - U_j''(y)\right].$$

The solution of problem (16)–(17) on each element is represented as a series in Chebyshev polynomials of the first kind

$$\psi_j(y) = \sum_{n=0}^{p_j} a_n^{(j)} T_n(y), \tag{19}$$

where $T_n(y)$ are Chebyshev polynomials of the first kind and $a_n^{(j)}$ are the unknown expansion coefficients.

Substituting this expansion into equation (18), we require the residual to be orthogonal to the first $(p_j - 4)$ Chebyshev polynomials. This gives the system of equations

$$\left(L_j\psi_j, T_n\right) = 0, \qquad n = 0,1,2,\ldots,p_j - 4; \qquad j = 1,2,\ldots,N. \tag{20}$$

To evaluate the term $U_j''(y)\psi_j(y)$ in the Orr–Sommerfeld operator, the second derivative of the base-flow velocity profile is obtained analytically from its Chebyshev expansion (11). The resulting coefficients are combined with the Chebyshev coefficients of the eigenfunction (19) using the multiplication properties of Chebyshev polynomials. This contribution is represented by the final double summation in Equation (21), thereby ensuring that the term $U_j''(y)\psi_j(y)$ is explicitly incorporated into the spectral discretization.

As a result, a system of algebraic equations is obtained for the coefficients $a_n^{(j)}$. System (20) can be written in the following form:

$$\begin{aligned}
&\frac{1}{24}\sum_{\substack{p=n+4\\ p\equiv n \pmod 2}}^{p_j}\left[p^3(p^2-4)^2 - 3n^2p^5 + 3n^4p^3 - pn^2(n^2-4)^2\right]a_p^{(j)}\\
&- 2k^2\sum_{\substack{p=n+2\\ p\equiv n \pmod 2}}^{p_j} p(p^2-n^2)a_p^{(j)} + k^4c_n a_n^{(j)}\\
&- \frac{1}{2}ik\mathrm{Re}\Bigg(\sum_{p=2}^{p_j} a_p^{(j)}\sum_{\substack{m\equiv p \pmod 2\\ |m|\le p-2\\ |n-m|\le p_j}} p(p^2-m^2)\bar{b}_{n-m}^{(j)}\\
&\qquad - k^2\sum_{\substack{|p|\le p_j\\ |n-p|\le p_j}}\bar{a}_p^{(j)}\bar{b}_{n-p}^{(j)}\\
&\qquad - \sum_{\substack{|p|\le p_j\\ |n-p|\le p_j}}\bar{a}_p^{(j)}\sum_{\substack{m=|n-p|+2\\ m+n\equiv p \pmod 2}}^{p_j} m\left[m^2-(n-p)^2\right]b_m^{(j)}\Bigg)\\
&- \lambda\left[ik^3\mathrm{Re}\,c_n a_n^{(j)} - ik\mathrm{Re}\sum_{\substack{p=n+2\\ p\equiv n \pmod 2}}^{p_j} p(p^2-n^2)a_p^{(j)}\right] = 0,\\
&\qquad\qquad n = 0,1,2,\ldots,p_j-4, \qquad j = 1,2,\ldots,N.
\end{aligned} \tag{21}$$

Here, $a_n^{(j)}$ and $b_n^{(j)}$ are the expansion coefficients of the functions ψ and U in Chebyshev polynomials. We also introduce the notation

$$\bar{a}_n^{(j)} = c_{|n|}a_{|n|}^{(j)}, \qquad \bar{b}_n^{(j)} = c_{|n|}b_{|n|}^{(j)}, \qquad -p_j \le n \le p_j,$$

where the coefficients c_n are defined as follows:

$$c_0 = 2, \qquad c_n = 1, \qquad n > 0.$$

Using expansion (19), the boundary and continuity conditions (17) are written as follows:

$$
\begin{aligned}
&\sum_{n=0}^{p_1}(-1)^n a_n^{(1)} = 0, \qquad \sum_{n=0}^{p_1}(-1)^{n-1} n^2 a_n^{(1)} = 0,\\
&\sum_{n=0}^{p_j} a_n^{(j)} = \sum_{n=0}^{p_{j+1}}(-1)^n a_n^{(j+1)},\\
&\frac{1}{l_j}\sum_{n=0}^{p_j} n^2 a_n^{(j)} = \frac{1}{l_{j+1}}\sum_{n=0}^{p_{j+1}}(-1)^{n-1} n^2 a_n^{(j+1)},\\
&\frac{1}{l_j^2}\sum_{n=0}^{p_j} a_n^{(j)} T_n''(+1) = \frac{1}{l_{j+1}^2}\sum_{n=0}^{p_{j+1}} a_n^{(j+1)} T_n''(-1),\\
&\frac{1}{l_j^3}\sum_{n=0}^{p_j} a_n^{(j)} T_n'''(+1) = \frac{1}{l_{j+1}^3}\sum_{n=0}^{p_{j+1}} a_n^{(j+1)} T_n'''(-1), \qquad j = 1, 2, \ldots, N-1,\\
&\sum_{n=0}^{p_N} a_n^{(N)} = 0, \qquad \sum_{n=0}^{p_N} n^2 a_n^{(N)} = 0.
\end{aligned}
\tag{22}
$$

Taking the continuity and boundary conditions (22) into account, system (21) gives a closed system of linear algebraic equations. The number of unknown coefficients in the resulting system is determined by

$$
\bar{m} = \sum_{j=1}^{N}(p_j + 1). \tag{23}
$$

The system of algebraic equations (21)–(22) can be written in matrix form

$$
(A - \lambda B)x = 0, \tag{24}
$$

where

$$
x^T = \left(a_0^{(1)}, a_1^{(1)}, \ldots, a_{p_1}^{(1)}, a_0^{(2)}, a_1^{(2)}, \ldots, a_{p_2}^{(2)}, \ldots, a_0^{(N)}, a_1^{(N)}, \ldots, a_{p_N}^{(N)}\right),
$$

where A and B are complex matrices of order $\bar{m} \times \bar{m}$, λ is the eigenvalue to be determined, and x is the vector of unknown coefficients.

The matrix B in system (24) is singular and contains $4N$ zero rows corresponding to the boundary and continuity conditions (22), because these conditions do not depend on λ.

To reduce the dimension of the system and identify the independent variables, elementary column transformations are applied to matrices A and B. As a result, the system is transformed into the equivalent form

$$
(AQ - \lambda BQ)(Q^{-1}x) = 0, \tag{25}
$$

or, introducing the notation

$$
Z = Q^{-1}x,
$$

we obtain

$$
(AQ - \lambda BQ)Z = 0. \tag{26}
$$

Here, Q is a nonsingular transformation that acts identically on matrices A and B. The vector Z has a block structure corresponding to the expansion of the solution in Chebyshev polynomials on the individual elements of the computational domain:

$$
Z^T = \left(0, 0, 0, 0, z_4^{(1)}, \ldots, z_{p_1}^{(1)}, 0, 0, 0, 0, z_4^{(2)}, \ldots, z_{p_2}^{(2)}, \ldots, 0, 0, 0, 0, z_4^{(N)}, \ldots, z_{p_N}^{(N)}\right).
$$

Since the same transformation Q is applied to both matrix A and matrix B, it is sufficient to describe the procedure for only one of them, with the analogous operations understood for the other. The transformation Q is selected to eliminate the unknowns associated with the boundary and continuity conditions. As a result, only the independent equations are retained from the full system, and the corresponding dependent components are eliminated.

For a computational domain divided into two elements ($N = 2$), the matrix A, which includes the spectral equations, boundary conditions, and coupling conditions at the element boundary, has the following structure:

$$A = \left(\begin{array}{cccccc|cccccc} 1 & -1 & 1 & -1 & \cdots & * & 0 & 0 & 0 & 0 & \cdots & 0 \\ 0 & 1 & -4 & 9 & \cdots & * & 0 & 0 & 0 & 0 & \cdots & 0 \\ * & * & * & * & \cdots & * & 0 & 0 & 0 & 0 & \cdots & 0 \\ \vdots & \vdots & \vdots & \vdots & & \vdots & \vdots & \vdots & \vdots & \vdots & & \vdots \\ * & * & * & * & \cdots & * & 0 & 0 & 0 & 0 & \cdots & 0 \\ 1 & 1 & 1 & 1 & \cdots & 1 & -1 & 1 & -1 & 1 & \cdots & * \\ 0 & 1 & 4 & 9 & \cdots & * & 0 & -1 & 4 & -9 & \cdots & * \\ 0 & 0 & 4 & 24 & \cdots & * & 0 & 0 & -4 & 24 & \cdots & * \\ 0 & 0 & 0 & 24 & \cdots & * & 0 & 0 & 0 & -24 & \cdots & * \\ 0 & 0 & 0 & 0 & \cdots & 0 & * & * & * & * & \cdots & * \\ \hline 0 & 0 & 0 & 0 & \cdots & 0 & \vdots & \vdots & \vdots & \vdots & & \vdots \\ 0 & 0 & 0 & 0 & \cdots & 0 & * & * & * & * & \cdots & * \\ 0 & 0 & 0 & 0 & \cdots & 0 & 1 & 1 & 1 & 1 & \cdots & * \\ 0 & 0 & 0 & 0 & \cdots & 0 & 0 & 1 & 4 & 9 & \cdots & * \end{array}\right).$$

To isolate the dependent components and subsequently reduce the order of the system, elementary column transformations of matrix A are performed using the nonsingular matrix Q. This gives the transformed matrix AQ of the following form:

$$AQ = \left(\begin{array}{cccccc|cccccc} 1 & 0 & 0 & 0 & \cdots & 0 & 0 & 0 & 0 & 0 & \cdots & 0 \\ 0 & 1 & 0 & 0 & \cdots & 0 & 0 & 0 & 0 & 0 & \cdots & 0 \\ x & x & x & x & \cdots & x & 0 & 0 & 0 & 0 & \cdots & 0 \\ \vdots & \vdots & \vdots & \vdots & & \vdots & \vdots & \vdots & \vdots & \vdots & & \vdots \\ x & x & x & x & \cdots & x & 0 & 0 & 0 & 0 & \cdots & 0 \\ 1 & 2 & 0 & 0 & \cdots & 0 & 0 & 1 & 0 & 0 & \cdots & 0 \\ 0 & 1 & 0 & 0 & \cdots & 0 & 0 & 0 & 1 & 0 & \cdots & 0 \\ 0 & 0 & 4 & 0 & \cdots & 0 & 0 & 0 & 0 & 0 & \cdots & 0 \\ 0 & 0 & 0 & 24 & \cdots & 0 & 0 & 0 & 0 & 0 & \cdots & 0 \\ 0 & 0 & 0 & 0 & \cdots & 0 & x & x & x & x & \cdots & x \\ \hline \vdots & \vdots & \vdots & \vdots & & \vdots & \vdots & \vdots & \vdots & \vdots & & \vdots \\ 0 & 0 & 0 & 0 & \cdots & 0 & x & x & x & x & \cdots & x \\ 0 & 0 & 0 & 0 & \cdots & 0 & 1 & 0 & 0 & 0 & \cdots & 0 \\ 0 & 0 & 0 & 0 & \cdots & 0 & 0 & 1 & 0 & 0 & \cdots & 0 \end{array}\right).$$

The structure of matrix AQ shows that, after the transformation, part of the equations corresponding to the boundary and coupling conditions becomes autonomous. This makes it possible to eliminate the corresponding dependent components and pass to a reduced eigenvalue problem of lower order.

The same transformation Q is applied to matrix B. As a result, matrix BQ is obtained, while the zero rows corresponding to the boundary and coupling conditions remain zero.

After these transformations, the system is reduced to the form

$$(T - \lambda W)\bar{Y} = 0, \tag{27}$$

where T and W are square matrices of lower order, and $\bar{Y}$ is the vector of independent unknowns. Since the total number of Chebyshev expansion coefficients is determined by relation (23), after eliminating four dependent components on each element, the order of the reduced matrices T and W becomes

$$(\bar{m} - 4N) \times (\bar{m} - 4N).$$

Thus, the dimension of the spectral-grid problem is substantially reduced, which makes the computation of the eigenvalues considerably more efficient.

To transform the generalized problem (27) into a standard problem, the transformation

$$D = TW^{-1}$$

is introduced. The standard eigenvalue problem is then considered instead of system (27):

$$(D - \lambda E)Y = 0. \tag{28}$$

This is the form used in the computational algorithm. After matrix D has been constructed, its spectrum can be obtained using standard numerical methods.

From the computed spectrum, the physically significant unstable mode corresponding to the largest positive value of the imaginary part of the eigenvalue λ_i is selected.

Thus, the computational procedure consists of a successive transition from the original generalized system (24) to the transformed system (26), then to the reduced system (27), and finally to the standard problem (28), whose solution yields the required eigenvalues and corresponding eigenvectors for the Orr–Sommerfeld problem.

Consequently, this transformation substantially reduces the order of the matrices in algebraic system (24) and improves computational efficiency. At the same time, the high accuracy of the spectral-grid approximation is preserved because transformation Q does not change the spectrum of the original problem.

After the eigenvalue λ has been computed, the corresponding eigenvector x of the original generalized system (24) must be reconstructed. Since the original problem (24) is successively transformed and reduced during the numerical solution, the vector x is not obtained directly;

instead, the eigenvector Y of the lower-order standard problem (28) is determined. Therefore, an inverse transformation procedure is required to obtain the eigenvector of the original system.

The procedure is performed as follows. First, from the standard problem

$$(D - \lambda E)Y = 0$$

the eigenvector Y is determined. Next, the reduced vector $\bar{Y}$ must be reconstructed. Since

$$D = TW^{-1},$$

the standard problem is equivalent to the system

$$(T - \lambda W)\bar{Y} = 0$$

under the substitution

$$Y = W\bar{Y}.$$

It follows that the reduced vector is reconstructed by the formula

$$\bar{Y} = W^{-1}Y.$$

Thus, the eigenvector obtained from the standard problem is transferred to the space of unknowns of the reduced system.

At the next stage, the complete transformed vector Z must be reconstructed. During the reduction, the components corresponding to the boundary and continuity conditions are removed from the original system. After transformation Q is applied, these components are placed at the beginning of vector Z and assigned zero values. If the integration domain is divided into N elements, the number of such zero components is $4N$, because four unknowns associated with the boundary and continuity conditions are eliminated on each element.

After the complete transformed vector Z has been constructed, the eigenvector of the original system can be recovered. Since

$$Z = Q^{-1}x,$$

the inverse transformation has the form

$$x = QZ.$$

The vector x obtained in this way is the eigenvector of the original system (24).

Because an eigenvector is defined up to an arbitrary nonzero multiplier, it is normalized with respect to the Euclidean norm before the eigenfunction is reconstructed:

$$\|x\|_2 = 1.$$

Thus, the eigenvector reconstruction algorithm consists of a successive transition from the eigenvector of the standard problem Y to the reduced vector $\bar{Y}$, then to the complete transformed vector Z, and finally to the eigenvector of the original system x.

The reconstructed eigenvector x contains the expansion coefficients of the eigenfunction ψ in Chebyshev polynomials. The values of function ψ at the spectral-grid nodes are calculated from these coefficients using expansion (19).

The resulting eigenvector makes it possible to reconstruct the structure of the perturbed flow and investigate the spatial distribution of the eigenfunctions. On the basis of vector x, plots of the perturbation function and its derivatives can be constructed, enabling a physical analysis of the characteristics of unstable flow modes.

After the eigenvalue λ and the corresponding eigenvector x have been found, the streamfunction amplitude ψ and its derivatives are reconstructed. The components of vector x are treated as the expansion coefficients of function ψ in Chebyshev polynomials of the first kind. Therefore, function $\psi(y)$ on the standard interval $y \in [-1, 1]$ is represented by series (19).

The collocation nodes of the Chebyshev polynomials, determined by relation (10), are used to calculate the function values. Substituting the node coordinates y_l into the Chebyshev expansion gives the values of the streamfunction amplitude at the nodes according to relation (19).

Thus, the dynamics of the velocity vector in the Navier–Stokes system is investigated according to the following sequence:

1. Equation (9) is solved using the fourth-order Runge–Kutta method, and the base-flow velocity profile in the boundary layer is determined on a uniform grid; the resulting velocity profile is then interpolated at the Chebyshev polynomial nodes (10).
2. The spectral-grid method is applied, with the base-flow velocity profile and the solution of the Orr–Sommerfeld equation (16) represented by the finite series (11) and (19), respectively.
3. Using the spectral-grid method, the continuous eigenvalue problem for the Orr–Sommerfeld equation is reduced to the generalized algebraic eigenvalue problem (20), (17).
4. System (24) is solved, and the eigenvalues λ and the corresponding eigenvectors (24) are obtained. The streamfunction amplitude (19) and its first derivative are then calculated from these vectors.
5. The velocity components of the perturbation motion are determined from (7).
6. The streamwise $u(x, y, t)$ and transverse $\vartheta(x, y, t)$ components of the velocity field are determined from formulas (2), taking into account the base flow and the linear perturbation.

4. Results

For the numerical investigation, the parameters $\mathrm{Re}_1 = 580$, $k_1 = 0.179$, and $\eta_{\max} = 20$ are fixed. The choice of these parameters is consistent with the results reported in [9]. The total number of spectral coefficients is set to $\bar{m} = 46$.

When a single element ($N = 1$) is used, the eigenvalue of the stability problem is computed. The obtained result is compared with the numerical value reported in [9]. The comparison is presented in Table 1.

Table 1. Comparison of the computed eigenvalues

Method	λ_r	λ_i	$\lvert\Delta\lambda_r\rvert$	$\lvert\Delta\lambda_i\rvert$
This study	0.36419492	0.00792907	–	–
Value reported in [9]	0.36412286	0.00795972	7.20×10^{-5}	3.06×10^{-5}

The influence of dividing the computational domain into several elements is then investigated. A two-element decomposition, $[0, 10]$ and $[10, \eta_{\max}]$, with $N = 2$, is considered. The parameters p_1 and p_2 characterize the polynomial approximation orders in the first and second elements, respectively. The first element is adjacent to the wall, where the base-flow profile and the corresponding eigenfunction exhibit stronger spatial variation. For some distributions of p_1 and p_2, the computational accuracy may be slightly lower than that obtained in the single-element case ($N = 1$).

Table 2. Influence of the number of polynomials on the computational accuracy

$p_1 + 1$	$p_2 + 1$	λ_r	λ_i	$\lvert\Delta\lambda_r\rvert$	$\lvert\Delta\lambda_i\rvert$
23	23	0.37184542	0.01451747	7.7×10^{-3}	6.5×10^{-3}
27	19	0.36295784	0.00853757	1.1×10^{-3}	5.7×10^{-4}
33	13	0.36418391	0.00793507	6.1×10^{-5}	2.4×10^{-5}

To further investigate the effect of subdividing the computational domain, a four-element case ($N = 4$) is considered with the total number of spectral coefficients fixed at $\bar{m} = 46$. The coefficients are redistributed among the elements without changing their total number.

Table 3. Influence of the distribution of polynomials among four elements on the computed eigenvalue

$p_1 + 1$	$p_2 + 1$	$p_3 + 1$	$p_4 + 1$	λ_r	λ_i	$\lvert\Delta\lambda_r\rvert$	$\lvert\Delta\lambda_i\rvert$
21	13	7	5	0.36495915	0.00706378	8.3×10^{-4}	8.9×10^{-4}
21	15	5	5	0.36394933	0.00782265	1.7×10^{-4}	1.3×10^{-4}
23	13	5	5	0.36416963	0.00787027	4.6×10^{-5}	8.9×10^{-5}
25	11	5	5	0.36422714	0.00792845	1.0×10^{-4}	3.1×10^{-5}
27	9	5	5	0.36422189	0.00792355	9.9×10^{-5}	3.6×10^{-5}

The results show that the accuracy of the computed eigenvalue depends not only on the total number of spectral coefficients but also on their distribution among the elements. Increasing the number of coefficients in the region where the solution profile varies more rapidly reduces the deviation from the reference value without increasing the overall approximation dimension.

The computational efficiency of the spectral-grid method can be assessed by the number of arithmetic operations required to solve the algebraic eigenvalue problem. For a complex matrix of order n, one step of the QR algorithm requires approximately

$$\bar{Q} \approx \frac{20}{3} n^3$$

arithmetic operations. Because domain subdivision and subsequent reduction decrease the order of the matrices solved in the spectral-grid method, the number of arithmetic operations is correspondingly reduced. A comparison of the computational costs of the spectral method (SM) and the spectral-grid method (SGM) for different values of the total number of spectral coefficients is given in Table 4.

Table 4. Comparison of the number of arithmetic operations for the spectral and spectral-grid methods

$\bar{m}$	SM	SGM	
	$\bar{Q}$	N	$\bar{Q}$
5	7	1	7
10	1440	2	53
20	27307	4	427
30	117173	6	1440
40	311040	8	3413
50	648907	10	6667
60	1170773	12	11520
70	1916640	14	18293
80	2926507	16	27307
90	4240373	18	38880
100	5898240	20	53333

As can be seen from Table 4, the difference in the number of arithmetic operations between SM and SGM becomes more pronounced as the total number of spectral coefficients $\bar{m}$ increases. This shows that reducing the matrix order in the spectral-grid method leads to a noticeable decrease in the computational cost of solving the eigenvalue problem.

To further assess the numerical accuracy of the proposed method, additional convergence tests were performed by varying the polynomial approximation orders and the computational domain length. Table 5 presents the corresponding eigenvalues, their deviations from the reference value, and the residuals of the differential operator and boundary conditions.

Table 5. Convergence and residual analysis of the selected eigenmode

$\eta_{\max}$	$p_1+1,\ p_2+1$	λ	$\lvert\Delta\lambda\rvert$	r_{OS}	$r_{\max}$
20	33, 13	$0.36418391 + 0.00793507i$	6.58×10^{-5}	4.34×10^{-2}	3.55×10^{-12}
20	43, 19	$0.36414448 + 0.00795330i$	2.26×10^{-5}	1.35×10^{-2}	1.06×10^{-10}
20	63, 31	$0.36414502 + 0.00795045i$	2.40×10^{-5}	3.03×10^{-4}	2.18×10^{-10}
25	43, 19	$0.36412496 + 0.00796218i$	3.24×10^{-6}	6.07×10^{-3}	5.68×10^{-11}
30	43, 19	$0.36411466 + 0.00796060i$	8.25×10^{-6}	2.80×10^{-3}	2.60×10^{-11}

Note. The reference eigenvalue is $\lambda_{\mathrm{ref}} = 0.36412286 + 0.00795972i$ [9]. Here, $|\Delta\lambda| = |\lambda - \lambda_{\mathrm{ref}}|$ denotes the absolute error of the complex eigenvalue, accounting for both its real and imaginary parts. The quantity r_{OS} represents the relative residual of the Orr–Sommerfeld differential operator, while $r_{\max}$ denotes the maximum residual of the boundary and continuity conditions. All computations were performed using two spectral elements with boundaries $(0, \eta_{\max}/2, \eta_{\max})$.

To construct the velocity-field components, a time instant $t = t_0$ is fixed. The streamwise and transverse components are calculated from the Blasius base-flow profile and the selected eigenmode of the Orr–Sommerfeld problem. The transverse coordinate is specified at the Chebyshev nodes $y_l = \cos(\pi l/p)$, $l = 0, 1, \ldots, p$, whereas the streamwise coordinate is selected on a uniform grid $x_k = 50k/p$, $k = 0, 1, \ldots, p$, over the interval $x \in [0, 50]$. The real and imaginary parts of the velocity-vector components $u(x, y, t_0)$ and $\vartheta(x, y, t_0)$ are presented as three-dimensional plots.

In Figures 1–4, the coordinate $y \in [-1, 1]$ is related to the physical transverse coordinate by $\eta = \eta_{\max}(1 + y)/2$. The plots represent complex velocity fields reconstructed from the normalized eigenmode with unit modal amplitude.

Three-dimensional plots of the real and imaginary parts of the streamwise velocity component are shown in Figures 1 and 2.

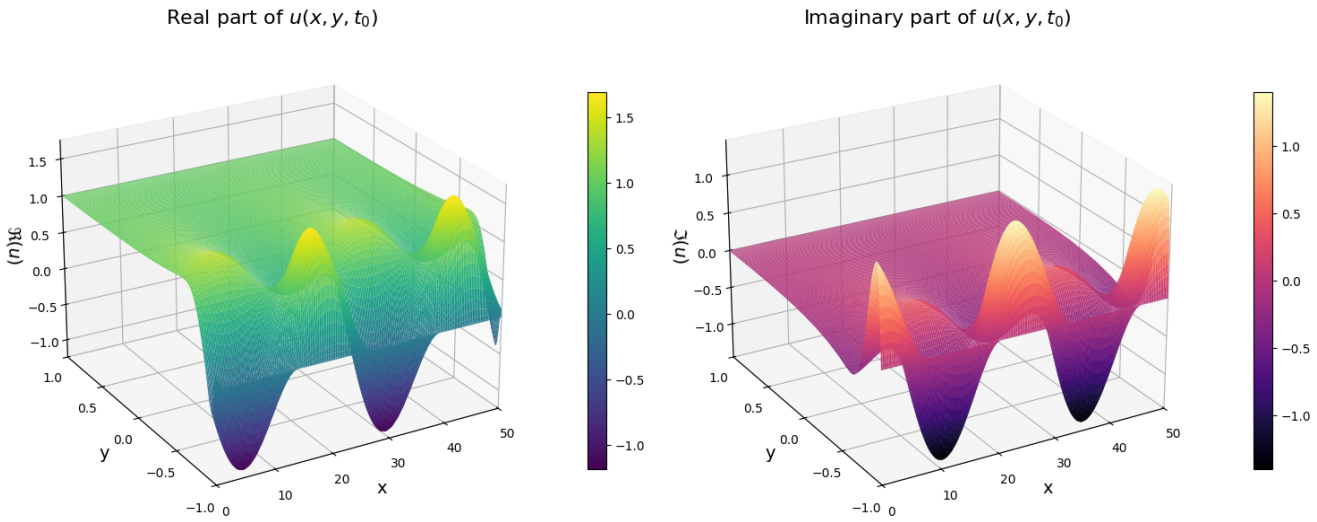


Figure 1. Real and imaginary parts of the streamwise velocity component $u(x, y, t_0)$ at $t_0 = 0$, computed over the domains $x \in [0, 50]$ and $y \in [-1, 1]$.

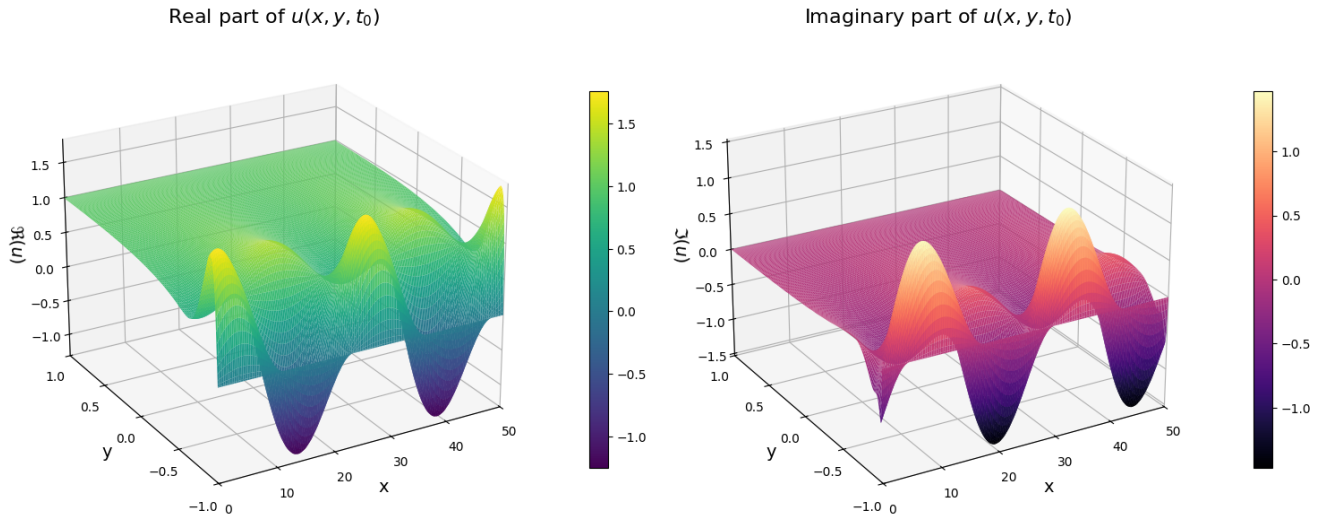


Figure 2. Real and imaginary parts of the streamwise velocity component $u(x, y, t_0)$ at $t_0 = 25$, computed over the domains $x \in [0, 50]$ and $y \in [-1, 1]$.

Three-dimensional plots of the real and imaginary parts of the transverse velocity component are shown in Figures 3 and 4.

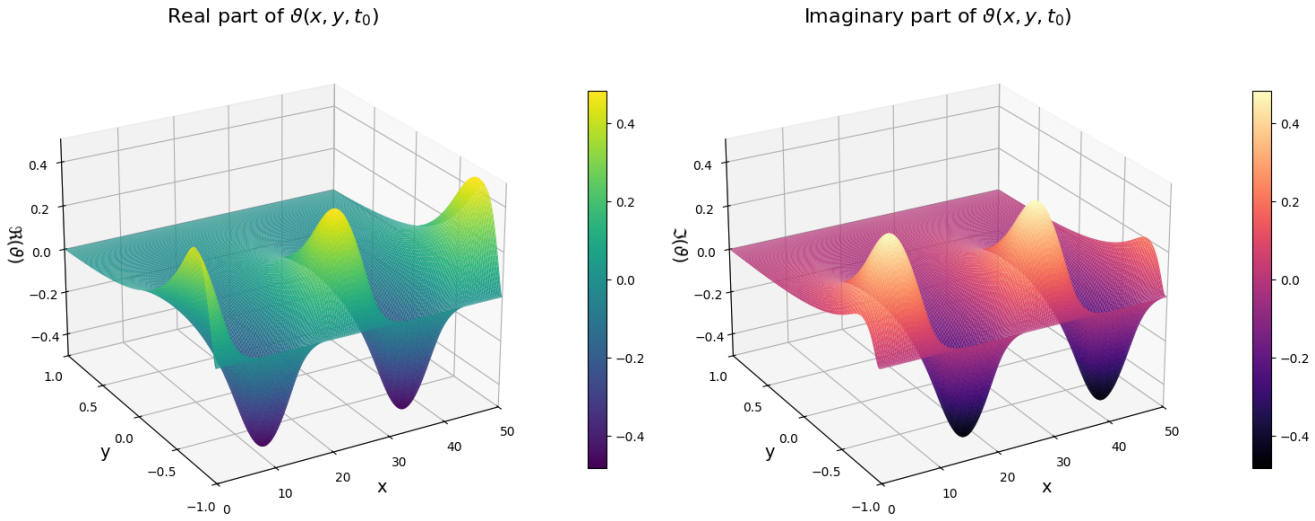


Figure 3. Real and imaginary parts of the transverse velocity component $\vartheta(x, y, t_0)$ at $t_0 = 0$, computed over the domains $x \in [0, 50]$ and $y \in [-1, 1]$.

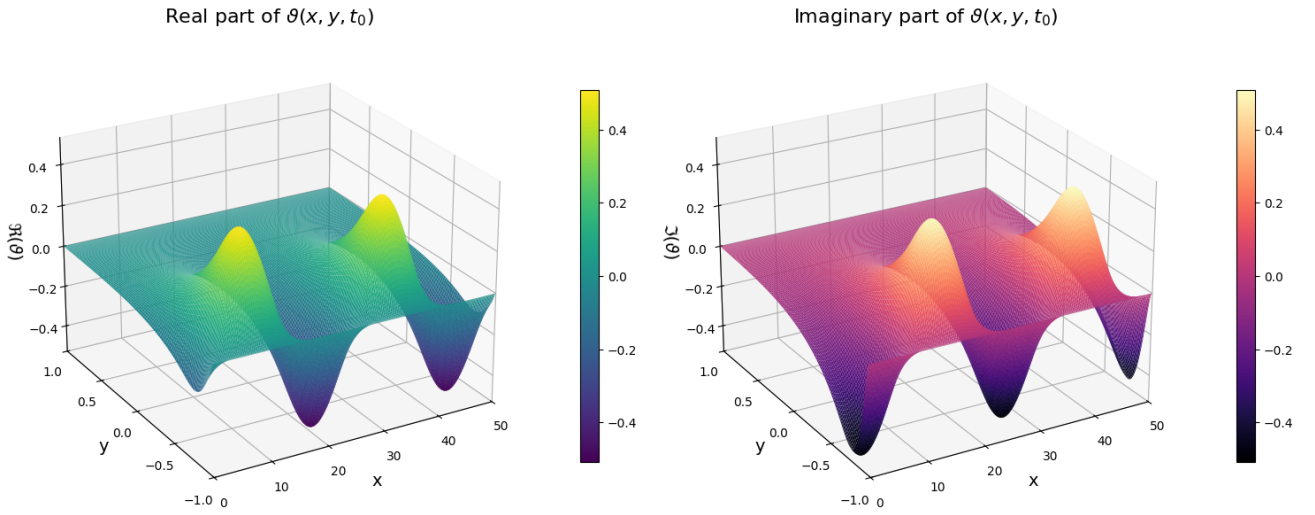


Figure 4. Real and imaginary parts of the transverse velocity component $\vartheta(x, y, t_0)$ at $t_0 = 25$, computed over the domains $x \in [0, 50]$ and $y \in [-1, 1]$.

A comparison of the results at $t_0 = 0$ and $t_0 = 25$ characterizes the temporal evolution of the selected eigenmode. The spatial structure of the streamwise and transverse perturbation components is generally preserved, whereas their amplitudes and phase positions change with time. Since $\lambda_i > 0$, the perturbation amplitude increases according to the law $e^{k\lambda_i t} = e^{k\,\mathrm{Im}(\lambda)t}$, which corresponds to the linear stage of the development of an unstable perturbation. The real and imaginary parts represent two phase components of the complex modal solution.

5. Conclusion

The following results were obtained from the linear stability analysis of the Blasius boundary layer and the reconstruction of the corresponding velocity-field components:

1. The base-flow velocity profile in the boundary layer is defined as the first derivative of the solution of the Falkner–Skan equation.
2. The differential eigenvalue problem for the Orr–Sommerfeld equation is reduced to a generalized algebraic eigenvalue problem by the spectral-grid method.
3. The streamfunction amplitude is a solution of the Orr–Sommerfeld equation and is expanded as a finite series in Chebyshev polynomials of the first kind with unknown coefficients.
4. The algebraic eigenvalue problem is solved, and the eigenvalues and corresponding eigenvectors (the unknown expansion coefficients) are obtained.
5. The streamfunction amplitude and its first derivative are calculated.
6. The velocity components of the perturbation flow are determined using the streamfunction.
7. The dynamics of the streamwise and transverse components of the Navier–Stokes velocity vector are investigated through the components of the perturbation-flow velocity vector, and their graphs are constructed.

8. As time increases, the amplitudes of the perturbations of the streamwise u and transverse ϑ velocity components increase exponentially, indicating temporal instability of the flow.

Declarations

Author Contributions: Conceptualization, Ch.N. and M.T.; methodology, Ch.N., M.T. and S.M.; software, M.T. and S.M.; validation, Ch.N., M.T., S.M. and R.A.; formal analysis, Ch.N., M.T. and N.D.; investigation, M.T., S.M. and R.A.; data curation, M.T. and S.M.; writing—original draft preparation, M.T.; writing—review and editing, Ch.N., M.T., R.A. and N.D.; visualization, M.T. and S.M.; supervision, Ch.N.; project administration, Ch.N. All authors have read and agreed to the published version of the manuscript.

Funding: This research received no external funding.

Ethics Approval: Not applicable.

Informed Consent and Consent for Publication: Not applicable.

Data Availability Statement: The data supporting the findings of this study are available from the corresponding author upon reasonable request.

Acknowledgments: The authors acknowledge the use of artificial intelligence (AI) tools to assist in translating the manuscript from Russian into English and converting the text and mathematical expressions into LaTeX format. The authors reviewed and verified the translated and formatted content and take full responsibility for the accuracy and scientific content of the manuscript.

Conflicts of Interest: The authors declare no conflicts of interest.

Nomenclature and Abbreviations

x, y	streamwise and transverse coordinates
u, ϑ	streamwise and transverse velocity components
$U(y)$	streamwise velocity of the base flow
$\widetilde{u}, \widetilde{\vartheta}$	small perturbations of the velocity components
$\psi(y)$	streamfunction amplitude
k	wavenumber
ω	complex frequency
λ	complex eigenvalue / phase velocity
λ_r, λ_i	real and imaginary parts of λ
Re	Reynolds number
β	Falkner–Skan pressure-gradient parameter
SGM	spectral-grid method
SM	spectral method

References

[1] Shoukat Z, Siddiqui AA, Yaseen MH, et al. An approximate solution of the Blasius problem using spectral method. *Partial Differ Equ Appl Math.* 2024;11:100896. https://doi.org/10.1016/j.padiff.2024.100896.

[2] Rahman MM, Khan S, Akbar MA. Numerical and analytical solutions of new Blasius equation for turbulent flow. *Heliyon.* 2023;9(3):e14319. https://doi.org/10.1016/j.heliyon.2023.e14319.

[3] Van Stijn TL, Van De Vooren AI. An accurate method for solving the Orr–Sommerfeld equation. *J Eng Math.* 1980;14:17–26. https://doi.org/10.1007/BF00042862.

[4] Dholey S. Unsteady boundary layer flow and heat transfer of a viscous fluid over a semi-infinite stationary flat plate: Blasius flow problem. *Phys Scr.* 2021;96(2):025204. https://doi.org/10.1088/1402-4896/abcd69.

[5] Fazio R. Free boundary formulations for two extended Blasius problems. *Int J Non-Linear Mech.* 2023;153:104423. https://doi.org/10.1016/j.ijnonlinmec.2023.104423.

[6] Al-Khaled K, Ajeel MS, Darweesh A, Al-Khalid H. A reliable algorithm for solving Blasius boundary value problem. *Results Nonlinear Anal.* 2024;7(4):1–8. https://doi.org/10.31838/rna/2024.07.04.001.

[7] Zubarev VM. Analytical approximation of solutions to the Blasius problem in the boundary layer on a flat plate. *Uchenye Zapiski Kazanskogo Universiteta. Seriya Fiziko-Matematicheskie Nauki.* 2025;167(2):227–243. (In Russ.). https://doi.org/10.26907/2541-7746.2025.2.227-243.

[8] Zubarev VM. Accurate analytical solutions of the velocity profile in the boundary layer on a plate (Blasius problem). *J Eng Phys Thermophys.* 2025;98(3):644–654. https://doi.org/10.1007/s10891-025-03144-9.

[9] Grosch CE, Orszag SA. Numerical solution of problems in unbounded regions: coordinate transforms. *J Comput Phys.* 1977;25(3):273–295. https://doi.org/10.1016/0021-9991(77)90102-4.

[10] Normurodov ChB, Tursunova BA. Numerical modeling of the boundary value problem of an ordinary differential equation with a small parameter at the highest derivative by Chebyshev polynomials of the second kind. *Results Appl Math.* 2023;19:100388. https://doi.org/10.1016/j.rinam.2023.100388.

[11] Normurodov Ch, Djurayeva N, Deraman F, Mat Safar A, Mohd Asi S. One effective method for solving singularly perturbed equations. *Malays J Sci.* 2025;44(1):63–69. https://doi.org/10.22452/mjs.vol44no1.8.

[12] Normurodov ChB, Solov'ev AS. Stability of two-phase gas-solid particle flow in a boundary layer. *Fluid Dyn.* 1987;22(2):217–221.

https://doi.org/10.1007/BF01052251.

[13] Normurodov ChB, Solov'ev AS. Effect of suspended particles on the stability of plane Poiseuille flow. *Fluid Dyn.* 1986;21(1):38–44. https://doi.org/10.1007/BF01051098.

[14] Normurodov ChB, Ziyakulova ShA, Murodov SK. On one highly accurate and efficient method for solving the biharmonic equation. *Int J Appl Math.* 2025;38(4):437–453. https://doi.org/10.12732/ijam.v38i4.1.

[15] Normurodov ChB, Djuraeva NT, Normatova MM. A highly accurate and efficient method for studying the dynamics of derivatives of different orders of a singularly perturbed equation. *Chebyshevskii Sbornik.* 2025;26(4):357–369. (In Russ.). https://doi.org/10.22405/2226-8383-2025-26-4-357-369.

Disclaimer of Liability/Publisher's Note

The statements, opinions, and data contained in all publications are solely those of the individual author(s) and contributor(s) and do not necessarily reflect the views of the Publisher, the Journal, or the editors. The Publisher, the Journal, and the editors disclaim responsibility for any injury to persons or damage to property resulting from any ideas, methods, instructions, or products referred to in the content.